The Solution Conformation of (D)Phe-Pro-Containing Peptides: Implications on the Activity of Ac-(D)Phe-Pro-boroArg-OH,[1] a Potent Thrombin Inhibitor

Marguerita S. L. Lim[†,‡], Eric R. Johnston,[§] and Charles A. Kettner*[,†]

The Du Pont Merck Pharmaceutical Company, and Central Research & Development Department, Du Pont Company, Experimental Station, Wilmington, Delaware 19880-0328

Received November 25, 1992

Ac-(D)Phe-Pro-boroArg-OH is a potent, competitive inhibitor of thrombin (K_i = 40 pM). ^{1}H-NMR studies have shown that the peptide portion, -(D)Phe-Pro-, has secondary structure in aqueous solutions. This structure corresponds fairly closely to the structure of H-(D)Phe-Pro-ArgCH_2Cl complexed to thrombin in the protein crystal structure (Bode, W.; et al. *EMBO J.* **1989**, *193*, 3467-3475.). These results indicate that, in addition to enthalpic interactions in the active site of the enzyme, there are significant entropic advantages in binding this molecule not previously recognized. We estimate that they contribute ~10-fold to binding. The structure we have observed can be explained by π-π interactions between the phenyl side chain of (D)Phe and the (D)Phe-Pro peptide bond. Assignment of structure is based first on the 0.8-1.2 ppm difference between the two Pro C$^\delta$ protons. The magnitude of these chemical shifts are consistent with aromatic ring current-induced effects expected for distances in our structure. The structure was further defined by interproton distances and correlation times calculated by backtransformation and correction of the NOESY and ROESY data to the longitudinal and transverse cross relaxation rates. Analysis of the vicinal coupling constants show that Phe χ_1 is not fixed. Correlation times for the peptide side chains and backbone indicate that the phenyl ring and boroArg side chain possess various degrees of internal motion, and that the rest of the peptide has a fairly rigid conformation.

Introduction

The specificities of proteases for peptides and inhibitors have been the subject of many studies. Effects of changes in amino acid residues of substrates and inhibitors on binding in the P_3 through P_3' sites have been determined[2] and interpreted at the level of interactions with residues comprising the active sites of the enzyme. Little attention has been given to the conformation of substrates and inhibitors in solution. In general, it has been assumed that there is no structure associated with small acyclic peptides and peptide analogs. This is not the case for a series of thrombin inhibitors with the -(D)Phe-Pro-boroArg- sequence.[3] In this paper, we characterize the secondary structure associated with this sequence by a modification of the NMR method originally proposed by Davis.[4] In addition, we provide evidence that this secondary structure contributes to the effectiveness of the inhibitor.

Many of the more effective inhibitors and substrates of thrombin share the -(D)Phe-Pro-Arg- sequence.[5] For example, we have reported that peptide boronic acids with the -(D)Phe-Pro-boroArg- are highly effective, reversible inhibitors of thrombin.[3] These compounds are slow-binding inhibitors which selectively inhibit thrombin with K_i's of 40 to <4 pM. More recently, we have demonstrated that Ac-(D)Phe-Pro-boroArg-OH is effective in the *in vivo* inhibition of thrombin, inhibiting both venous and arterial thrombosis[6] following administration by a number of different routes.[7]

At the molecular level, substantial information is available for the interaction of this inhibitor with thrombin. The crystal structure of thrombin complexed with H-(D)Phe-Pro-ArgCH_2Cl[5a,b] has been determined and as expected (D)Phe and Pro occupy the P_3 and P_2 binding sites.[8] The arginyl side chain binds in the primary site with the carbonyl moiety in a tetrahedral complex with the active-site serine; the active-site histidine is alkylated by the chloromethyl ketone portion of the molecule. We would predict that peptide boronic acids with this sequence would behave similarly, except the boronic acid would form a reversible tetrahedral complex with the active site serine. This is based on earlier NMR[9] and X-ray crystallographic[10] studies with α-lytic protease and peptide boronic acid elastase inhibitors. This mode of binding has been confirmed recently for the binding to thrombin[11].

Furthermore, the conformation of the -(D)Phe-Pro- portion of H-(D)Phe-Pro-ArgCH_2Cl complexed to thrombin is very similar to the solution structure of Ac-(D)Phe-Pro-boroArg-OH we have determined. The entropic advantage of receptors binding conformationally-restricted molecules has been recognized for some time.[12] Conformational restriction by steric hindrance and cyclization have increased the activity and selectivity of linear peptide hormones and neurotransmitters toward receptors.[13] The similarity between free and bound forms of Ac-(D)Phe-Pro-boroArg-OH has provided a unique opportunity to compare the effect of inhibitor solution structure on binding to an enzyme.

Results

Assignment of Proton Signals. Prior to quantitative measurements of the NOEs between the protons of interest, the ^{1}H-NMR signals were assigned for **I** with 2D COSY (Figure 1), TOCSY, NOESY, and heteronuclear ^{1}H-^{13}C correlation experiments (not shown here). Two sets of signals were observed for Phe C$^\alpha$H and Pro C$^\alpha$H, corresponding to the *cis* and *trans* isomers of the (D)Phe-Pro peptide bond. Extremely strong NOEs between one of the Phe C$^\alpha$H signals and both Pro C$^\delta$H(*pro-S*) and (*pro-*

*Author to whom correspondence should be addressed.
† The Du Pont Merck Pharmaceutical Co.
‡Presently at Corvas International, 3030 Science Park Rd., San Diego, CA 92121.
§ Du Pont Co.

0022-2623/93/1836-1831$04.00/0

Table I. Pro C$^{\delta}$H Chemical Shift Nonequivalence of I and Analogs of I[a]

peptide	solvent	Pro C$^{\delta}$Hδ chemical shift δ (ppm) pro-*R*	pro-*S*	chemical shift difference, $\Delta\delta$ (ppm)
I, Ac-(D)Phe-Pro-boroArg-OH	D_2O	2.68	3.68	1.00
II, Boc-(D)Phe-Pro-boroArg-OH	D_2O	2.95	3.65	0.70
	CD_3OD	2.90	3.65	0.75
III, H-(D)Phe-Pro-boroArg-OH	D_2O	2.77	3.53	0.76
IV, Ac-(D)Phe-Pro-boroIrg-OH	D_2O	2.74	3.64	0.90
	CD_3OD	2.68	3.67	0.99
	$CDCl_3/CD_3OD$ 1:1	2.52	3.64	1.12
	$CDCl_3/CD_3OD$ 3:1	2.47	3.65	1.18
Boc-(D)Phe-Pro-OH	CD_3OD	2.98	3.60	0.62
Ac-(D)Phe-Pro-OH	CD_3OD	2.86	3.66	0.80

[a] The chemicals shifts were measured from data acquired at 298 K on the GE QE-300, with a sweep width of 10 ppm, typically with a 3-s relaxation delay and a 30° pulse width. The free induction decays were averaged for at least 32 scans and no more than 96 scans, then transformed without apodization. The spectra were referenced to either tetramethylsilane in $CDCl_3$ and CD_3OD or 3-(trimethylsilyl)propionic acid-d_4 sodium salt in D_2O.

Scheme I

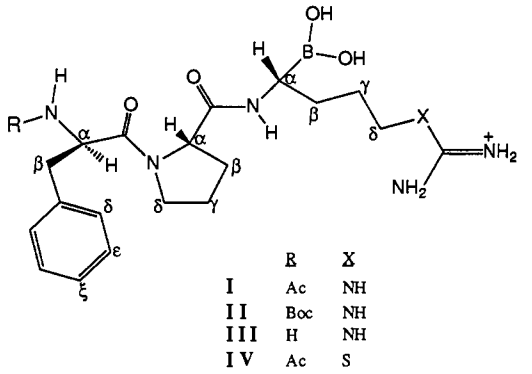

	R	X
I	Ac	NH
II	Boc	NH
III	H	NH
IV	Ac	S

R) resonances distinguished between Pro C$^{\alpha}$H/Phe C$^{\alpha}$H belonging to *trans* and *cis* isomers. The ratio of *cis* to *trans* as calculated from the peak area ratios for Phe C$^{\alpha}$H and Pro C$^{\alpha}$H was 1:20.

The chemical shift difference between Pro C$^{\delta}$H(*pro-R*) and Pro C$^{\delta}$H(*pro-S*) in **I** was about 1.0 ppm, depending on the solvent (Table I). Similar shift differences were observed for **II**, **III**, **IV**, and other (D)Phe-Pro-containing tripeptides. When there was no C-terminus substitution on the proline residue, the shift differences were substantially reduced, as found for the Boc- and Ac-protected dipeptides.

Solvent and Temperature Perturbations. The magnetic nonequivalence of Pro C$^{\delta}$H(*pro-R*) and Pro C$^{\delta}$H(*pro-S*) increased with greater solvent hydrophobicity. Higher percentages of CD_3OD in D_2O increased the separation from 0.90 to 1.00 ppm; increasing hydrophobicity with additions of $CDCl_3$ to **IV** in CD_3OD also continued the trend.

Temperature perturbation of the frequency separation was also studied. Pro C$^{\delta}$Hs showed coefficients of only −0.5 and 1.6 ppb/K, respectively (Figure 2). This suggests that no great conformational changes occur with lower temperature. The temperature coefficients of the (D)Phe and boroArg amide protons were, respectively, −8.5 and −10.0 ppb/K, indicating the absence of hydrogen bonding.[14] Varying pH and addition of 6 M urea did not significantly affect the chemical shifts of the analogs (data not shown).

Coupling Constants and Rotamer Analysis of the (D)Phe Residue. Table II gives the dihedral angles between vicinal protons obtained from their scalar coupling constants.[15] Peaks for Phe C$^{\alpha}$H, Phe C$^{\beta}$H(downfield), and Phe C$^{\beta}$H(upfield), in **I**, were well resolved at 4.78, 3.14, and 2.90 ppm, respectively. The vicinal coupling constants $^3J_{\alpha\beta}$(downfield) and $^3J_{\alpha\beta}$(upfield) describing the two

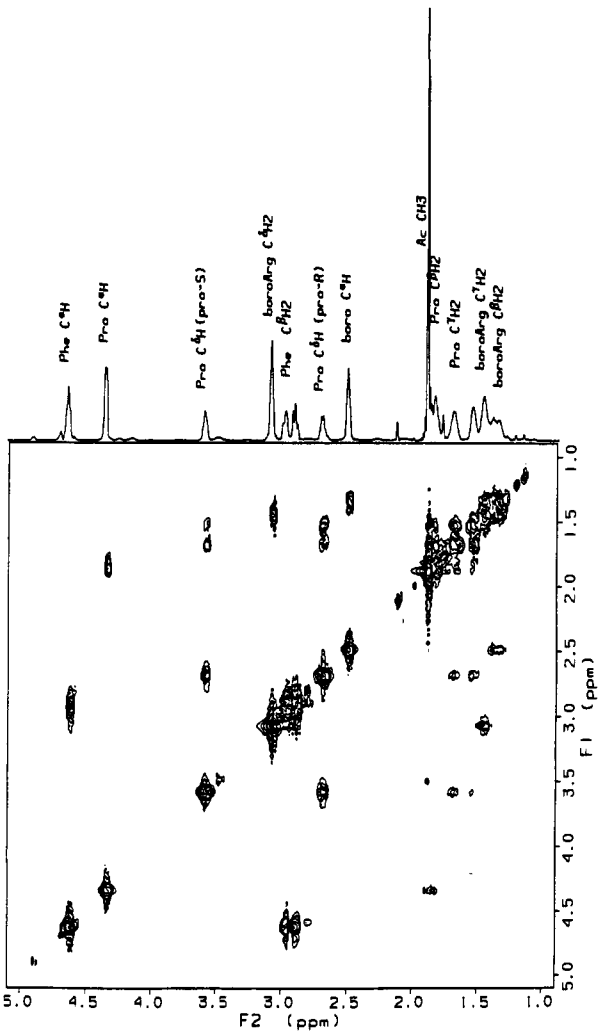

Figure 1. Two-dimensional COSY on Ac-(D)Phe-Pro-boroArg-OH (**I**). **I** was analyzed as a 10 mM solution in D_2O. The data was acquired through a Bruker AMX600, with 96 scans for each of the 1024 increments in the COSY experiment using the procedure of Aue et al.[35] The spectra are shown in magnitude mode.

dihedral angles Phe H–C$^{\alpha}$–C$^{\beta}$–H(downfield) and Phe H–C$^{\alpha}$–C$^{\beta}$–H(upfield), respectively, were obtained from spectral simulations of the peaks. These were correlated with chemical shift changes to specifically assign Phe Hβ(*pro-S*) and Phe Hβ(*pro-R*), allowing Phe χ_1 to be deduced.

At lower temperatures, $^3J_{\alpha\beta}$(upfield) increased, in conjunction with increasing Pro C$^{\delta}$H anisotropy. The first

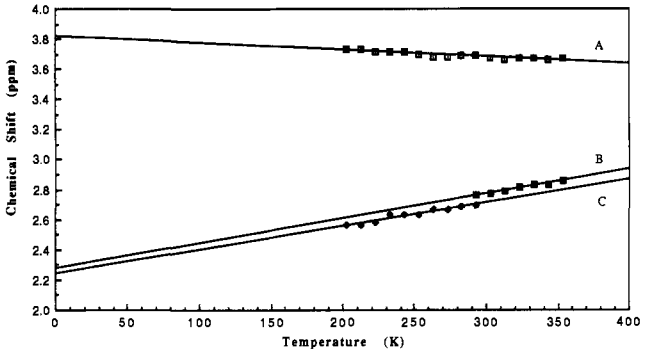

Figure 2. Temperature perturbation of the chemical shift difference between Pro $C^{\delta}H(pro\text{-}R)$ and Pro $C^{\delta}H(pro\text{-}S)$ in Ac-(D)Phe-Pro-boroArg-OH (I). Measurements at 295 K and higher temperatures were made in D_2O solutions of I (10 mM), measurements were also made at and below 295 K in CD_3OD solutions of I (10 mM). The gradients of the lines were calculated by linear regression to be −0.5 ppb/K for curve A [Pro $C^{\delta}H(pro\text{-}S)$], 1.6 ppb/K for curve B [Pro $C^{\delta}H(pro\text{-}R)$, I in D_2O], and 1.6 ppb/K for curve C [Pro $C^{\delta}H(pro\text{-}R)$, I in CD_3OD]. The acquisition parameters were as given in Table I.

effect suggests that Phe $C^{\beta}H$(upfield) was increasingly *trans* to Phe $C^{\alpha}H$. The aromatic ring adjacent to the Pro ring accounts for the second observation and is best accommodated when χ_1 is 180° as in rotamer I (Figure 3), whereby $^3J_{\alpha\beta}(pro\text{-}R)$ would be larger than $^3J_{\alpha\beta}(pro\text{-}S)$. Therefore, we assigned the smaller vicinal coupling constant to $^3J_{\alpha\beta}(pro\text{-}S)$ and the larger to $^3J_{\alpha\beta}(pro\text{-}R)$ (Table II).

For I, $^3J_{\alpha\beta2}$ and $^3J_{\alpha\beta3}$ gave χ_1 values which are obviously incompatible. This rules out the single conformation model for the (D)Phe side chain. We estimated the rotamer populations (Table II) for each of three values of Phe χ_1 corresponding to three staggered rotamers about χ_1 (Figure 3), bearing in mind that ±0.3 Hz errors in coupling constants may lead to as much as 8% errors in estimating rotamer populations.[16]

Rotamer analysis of Phe $^3J_{\alpha\beta2}$ and $^3J_{\alpha\beta3}$ gives the populations (Figure 3) of rotamer I (χ_1 = 180°), rotamer II (χ_1 = 60°), and rotamer III (χ_1 = −60°) as 75–80%, 20–25%, and 0%, respectively. The population P_I for rotamer I ranged from 65 to 85% with decreasing temperatures (353–293 K). Although these numbers seem plausible, Phe χ_1 may be better described by two much more closely related values, as suggested by solution structure deduced from the NOE and ROE data (Figure 5 and later discussion).

Nuclear Overhauser Effects. Conformational folding may be observed by dipole–dipole relaxation between protons close together in space. Dipolar coupling is detected by experiments such as 2D NOESY or ROESY. The tripeptide Ac-(D)Phe-Pro-boroArg-OH has 18 sets of equivalent spins from nonexchangeable protons in the predominant *trans* isomer. The presence of the minor *cis* isomer was irrelevant as no *cis*/*trans* exchange crosspeaks were detected in either NOESY or ROESY experiments, indicating extremely slow isomerization. No interactions were observed for the acetyl protons. The 2D ROESY and NOESY spectra of I were thus represented as two 18 × 18 matrices of peak volumes, mostly symmetrical although the spectra were not symmetrized. Peak intensities for (i,j) and (j,i) pairs were not averaged. Tabulated values of $\mathbf{A}_{\parallel}$, $\mathbf{A}_{RF}$, $\mathbf{R}_{\parallel}$, $\mathbf{A'}_{RF}$, $\mathbf{R}_{RF}$, and $\mathbf{R}_{\perp}$ are given in the supplementary material. NOESY and ROESY crosspeaks for key (D)Phe and Pro connectivities are shown in Figure 4.

Molecular Model. Interproton distances and correlation times for proton pairs were calculated by back-transformation and correction of the NOESY and ROESY data to the longitudinal and transverse cross relaxation rates using the procedure described in the Experimental Section. These values are reported in Table IV. Ten different structures obtained from molecular dynamics simulations were minimized as described in the Experimental Section and the best solution structure is given in Figure 5. For this structure, the difference in total energy between minimizations with and without restraints was 0.08 kcal. The maximum distance violations were 0.25 and 0.22 Å for pairs F and J, respectively, for the first determination with restraints. For the second determination without restraints, these values were 0.35 and 0.36 Å, respectively. These small differences may be due to sampling different structural populations arising from proline ring puckering during NMR measurements.

Binding Constants for the Inhibition of Thrombin. The binding constants of a series of di- and tripeptide boroArg analogs with Gly in the P_2 position were determined and compared with those previously obtained for P_2-Pro inhibitors (Table III). Only Ac-(D)Phe-Pro-boroArg-OH and Boc-(D)Phe-Pro-boroArg-OH were slow-binding inhibitors, and the reported K_i's are the values measured at steady state. It should be noted that kinetic measurements were made on the pinanediol esters for the two Boc-protected inhibitors. As we have reported previously,[3] side-by-side comparisons of the free boronic acid and the pinanediol ester indicate identical behavior.

Discussion

Binding of Ac-(D)Phe-Pro-boroArg-OH to Thrombin. Contrary to the expected, we have shown that the -(D)Phe-Pro- portion of Ac-(D)Phe-Pro-boroArg-OH and similar molecules have secondary structure in solution. This structure is very similar to that of H-(D)Phe-Pro-ArgCH_2Cl bound in the active site of thrombin in the protein X-ray structure[8] (Figure 5). Binding interactions here have been explained mainly on the basis of enthalpic energies of binding, ΔH. In contrast, the association of structure with the inhibitor in solution and its compliance with the bound structure strongly suggest that the entropic term $T\Delta S$ is important in explaining the overall effectiveness of these molecules in binding thrombin.

$$\Delta G_{binding} = \Delta H - T\Delta S$$

Page and Jencks[12] estimate that restricting rotation about a single carbon–carbon bond of a ligand should increase binding by 4.5 entropy units, decreasing K_i approximately 10-fold.

We have attempted to quantity the conformational contribution by comparing I and II with the corresponding P_2 Gly inhibitors. Assuming that binding in the P_3 site is independent of the nature of the residue in the P_2 site, the contribution of Pro relative to Gly may be due to two effects: favorable hydrophobic interactions from the extra three methylene groups of Pro and conformational advantages over the -(D)Phe-Gly- sequence. The hydrophobic interaction contribution was estimated from the ratio of the K_i's for Ac-Gly-boroArg-OH and Ac-Pro-boroArg-OH to be almost 10-fold. The P_2 Pro tripeptides showed a 100-fold greater affinity than the P_2 Gly inhibitors for α-thrombin. Thus, a factor of 10 in binding may be

Table II. $^3J_{\alpha\beta}$ for Phe Hβ(pro-*S*) and Hβ(pro-*R*) for IV[a]

temperature (K)	solvent	peak splitting Hα-Hβ (Hz)		coupling constant $^3J_{\alpha\beta}$ (Hz)		dihedral angle θ (deg)		population (%)[b]		
		pro-*S*	pro-*R*	pro-*S*	pro-*R*	pro-*S*	pro-*R*	P_I	P_{II}	P_{III}
353	H_2O/D_2O 4:1	7.2	8.4	7.1	8.5	−132	138	65	35	0
333	H_2O/D_2O 4:1	6.9	8.7	6.7	8.9	−130	140	70	30	0
293	H_2O/D_2O 4:1	6.5	9.3	6.2	9.6	−128	144	75	25	0
293	CD_3OD	6.8	9.5	6.6	9.7	−130	145	80	20	0
293	$CDCl_3/CD_3OD$ 3:1	6.1	10.0	5.7	10.3	−125	150	85	15	0

[a] The data were acquired on a GE QE-300, with 0.1 Hz per data point resolution. The free induction decays were typically averaged over 32, 64, or 96 scans, and a 0.5-Hz resolution enhancement was applied before Fourier transformation. The coupling constants $^3J_{\alpha\beta(\text{pro-}S)}$ and $^3J_{\alpha\beta(\text{pro-}R)}$ were calculated from the peak splittings and chemical shifts by "LAOCOON5" spectral simulation (derived from Bothner-By and Castellano[34]). [b] The populations, for the rotamers I, II, and III in Figure 3, were calculated as given in eqs 2 and 3. The values were rounded to the nearest 5%.

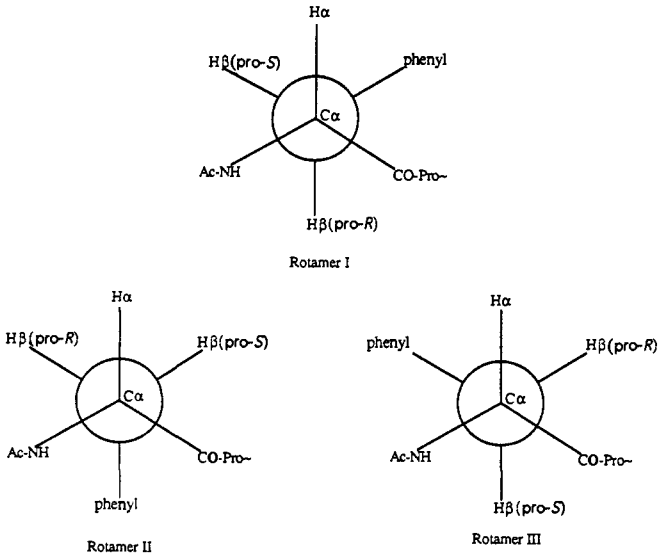

Figure 3. Newman projections of the three rotamers along Phe C^α–C^β.

attributable to conformation. We would have predicted a larger effect of conformation on the binding of the thrombin inhibitors. For example, if one predicts an increase in affinity of 10-fold due to stabilization of a single carbon–carbon bond, we would have predicted an increase in binding in the range of 3 orders in magnitude arising from the restricted conformation of the three carbon to carbon bonds between the carbonyl and aromatic ring of (D)Phe alone. However, we have not ruled out the possibility that there is structure associated with the dipeptide analogs and with the -(D)Phe-Gly-boroArg-OH peptides used for comparison or that there is interaction between the P_2 and P_3 binding sites. Alternatively, peptide inhibitor or substrate binding to serine proteases may be less dependent on solution structure than are agonist/receptor interactions. For thrombin, binding of the P_1 arginyl residue is required for activity while that of the P_2 and P_3 residues, -(D)Phe-Pro-, is of less importance in determining potency. One may envision binding occurring in two steps, in which the P_1 residue is bound first, acting as an anchor, and then the degrees of freedom for binding at the P_2 and P_3 sites are reduced.

Structure of Ac-(D)Phe-Pro-boroArg-OH in Solution. The complete assignment of the ^1H and ^{13}C spectra has been made. The magnitude of the Pro $C^\delta H$ anisotropy is 1 ppm instead of 0.03 ppm as expected for a "random coil" sequence.[17] The (D)Phe-Pro bond is predominantly *trans*, with 5% of the *cis* conformation present.

NOEs and ROEs were observed between (D)Phe and Pro residues, and within the boroArg side chain. The structural properties of the molecule were characterized from these data. It should be noted that structure is not usually associated with small acyclic peptides and that there are pitfalls in all structural assignments based on experimental NOE and ROE data. A solution structure

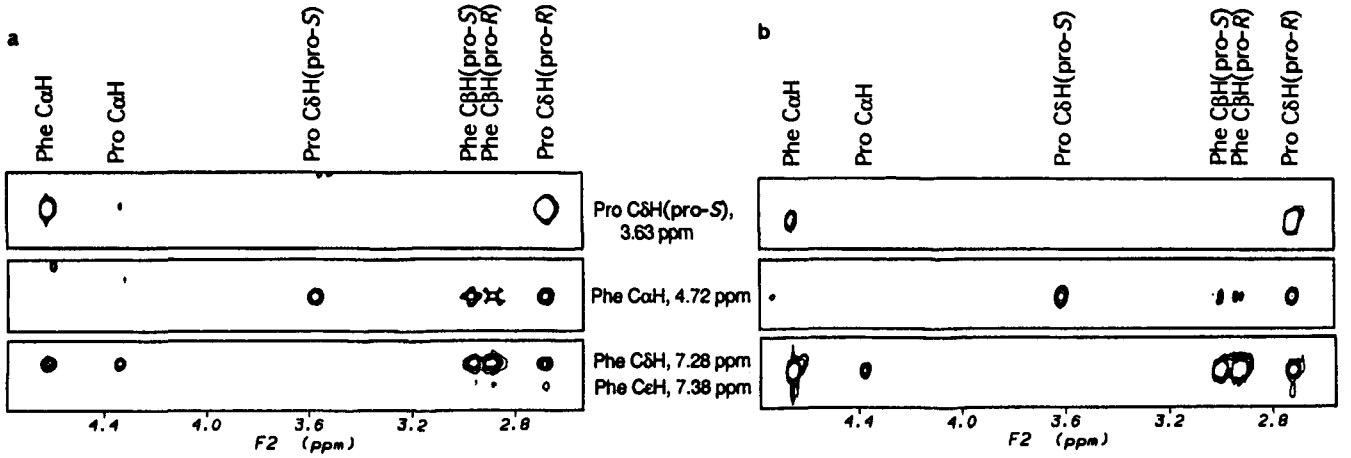

Figure 4. Two-dimensional (a) NOESY and (b) ROESY spectra of Ac-(D)Phe-Pro-boroArg-OH (I). The crosspeaks for both NOESY and ROESY were of opposite sign to the diagonal peaks. Only the negative peaks are shown. The NOESY and ROESY experiments were performed on an AMX600 with a previously degassed 2 mM solution of I in 99.996% D_2O, at 298 K. The mixing time of 600 ms was optimized from initial trials (0–700 ms in 100-ms steps). In the ROESY experiment a 2.6 kHz spin-lock was offset by 3 kHz downfield from the transmitter before the start of the mixing, then returned to the HOD peak before the free induction decay. The HOD peak was not presaturated. 96 scans, separated by delays of 5 s, were acquired for each of 1024 t_1 increments. Data were collected in absorption mode using States-Haberkorn-TPPI, and was zero-filled in the t_1 time domain to give a 2K × 2K matrix. Each domain was multiplied by a squared cosine bell before transformation.

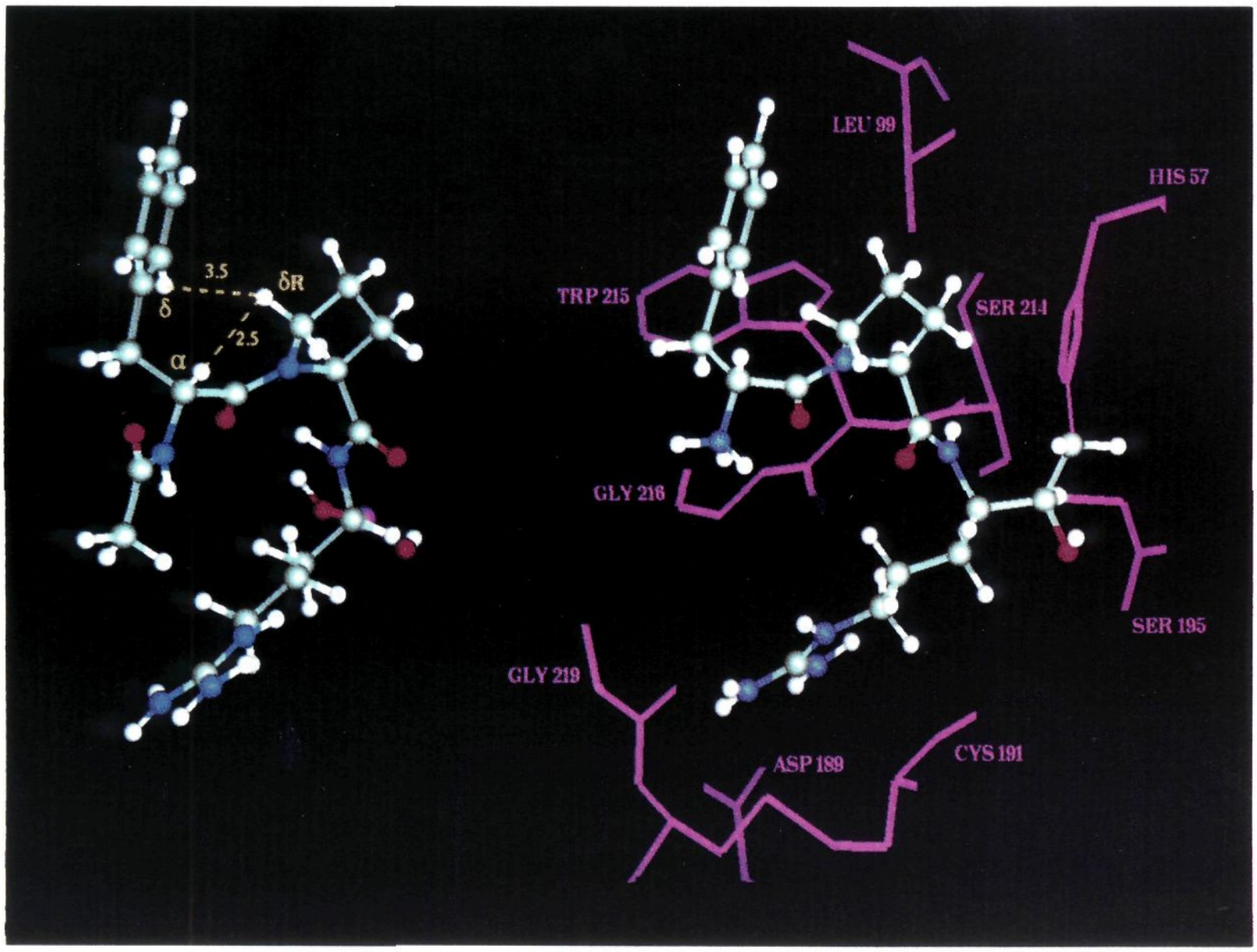

Figure 5. Comparison of the solution structure of Ac-(D)Phe-Pro-boroArg-OH with the conformation of H-(D)Phe-Pro-ArgCH_2Cl bound to thombin. The solution structure of **I**, developed by applying distance restrains in Table IV and energy minimization, is shown on the left. The structure of H-(D)Phe-Pro-Arg-CH_2Cl bound in the active site of thrombin is on the right. For alignment of the two structures, the phenyl rings were superimposed. Carbons and bonds are shown in green. Hydrogens, nitrogens, oxygens, and boron are white, blue, red, and pink, respectively. For the H-(D)Phe-Pro-ArgCH_2Cl:thrombin complex, portions of the enzyme are given in purple and enzyme residues are numbered according to the chymotrypsin numbering system. Note that no conformation is assigned to the arginyl side chain of the solution structure and the shown structure is only due to energy minimization. See Table IV footnotes for measured interproton distances for both structures.

Table III. Final Inhibition Constants for Binding with Thrombin[a]

inhibitor	K_i (pM)	contribution of P_2 Pro[b]
Ac-Gly-boroArg-OH	26000 ± 1000	
Ac-Pro-boroArg-OH	3300 ± 1400	7.9
Ac-(D)Phe-Gly-boroArg-OH	4300 ± 1200	
Ac-(D)Phe-Pro-boroArg-OH, **I**[c]	41 ± 3	105.0
Boc-(D)Phe-Gly-boroArg-OH[d]	400 ± 10	
Boc-(D)Phe-Pro-boroArg-OH, II[c,d]	4.0 ± 0.6	100.0

[a] The kinetic values were determined as described previously,[3] in 100 mM sodium phosphate buffer, pH 7.5, containing 200 mM NaCl and 0.5% polyethylene glycol 6000. Reported values with standard deviations are the average of at least two measurements. Human α-thrombin (specific activity 2340 NIH units/mg) at a level of 0.2 nM and the chromogenic substrate, H-(D)Phe-Pip-Arg-*p*NA (S2238), over a range of 200–20 μM, were used. [b] The contribution of Pro in the P_2 position was obtained by dividing the final inhibition constant for the P_2 inhibitor by that for the corresponding P_2 Gly analog. [c] Kinetic constants for **I** and **II** have been reported previously.[3] These are slow-binding inhibitors and the reported K_i values are those measured at the steady state. The remaining inhibitors are non-slow-binding. [d] Kinetic measurements for the Boc-protected inhibitors were made on the pinanediol esters, which have previously been shown to behave identically to the free boronic acids[3].

may be dismissed as that of an average or virtual conformation. Also, it is possible that only one structure among many in solution gives rise to observed NOEs. Even if there were only one solution structure, spin diffusion and internal motion may lead to a false interpretation of NOE measurements. The same is true for ROEs, in addition to the fact that the necessarily imperfect ROESY spin-lock distorts the ROE for each proton pair differently. To overcome these limitations, we experimentally determined both the structure and dynamics of **I** from the cross relaxation rates, without prior assumptions, and corrected these data for spin diffusion, the spin-lock field, and internal motion. The result is our model shown in Figure 5.

The (D)Phe-Pro bond is in the *trans* conformation, Phe ψ is 80–100°, and Phe χ_1 is 180°. The closest contacts between the two rings are from Phe $C^\delta H$ to Pro $C^\alpha H$, and to Pro $C^\delta H$(*pro-R*). There does not appear to be secondary structure associated with the Ac or Boc N-terminal groups, or the boroarginyl side chain (The structure of these groups as shown in Figure 5 is derived from energy minimizations). This model is supported by three main pieces of evidence: (1) the chemical shift differences between Pro $C^\delta Hs$, (2) interproton distances (Table IV), and (3) correlation times for the proton–proton vectors.

First, the large difference in chemical shifts for the Pro $C^\delta Hs$ is consistent with ring stacking in our model. Pro $C^\delta H$(*pro-R*) is near the 1 ppm diamagetic isoshielding line associated with the phenyl ring and Pro $C^\delta H$(*pro-S*) is in

Table IV. Correlation Times and Interproton Distances for I

	proton pair	correlation time (ns)[a]	^1H-^1H distances (Å)[b]
A[e]	Phe C$^\delta$H–Phe C$^\epsilon$H	0.08	2.3[d]
B	Phe C$^\beta$H(pro-*S*)–Phe C$^\delta$H	0.14, 0.18	2.5, 2.7
C	Phe C$^\beta$H(pro-*R*)–Phe C$^\delta$H	0.14, 0.18	2.5, 2.6
D	Phe C$^\alpha$H–Phe C$^\delta$H	0.17, 0.17	2.9[d]
E	Phe C$^\beta$H(pro-*S*)–Phe C$^\beta$H(pro-*R*)	0.16, 0.21	1.9, 2.0
F	Phe C$^\delta$H–Pro C$^\alpha$H	0.03	3.3[d]
G	Phe C$^\alpha$H–Pro C$^\delta$H(pro-*S*)	0.18, 0.23	2.2, 2.3
H	Phe C$^\alpha$H–Pro C$^\delta$H(pro-*R*)	0.20, 0.21	2.3, 2.4
I	Phe C$^\beta$H(pro-*S*)–Pro C$^\delta$H(pro-*R*)	0.19, 0.24	4.0, 4.2
J	Phe C$^\delta$H–Pro C$^\delta$H(pro-*R*)	0.21, 0.22	3.0, 3.1
K	Pro C$^\delta$H(pro-*S*)–Pro C$^\delta$H(pro-*R*)	0.22, 0.22	1.8
L	Pro C$^\alpha$H–Pro C$^\beta$H(pro-*S*)	0.21, 0.25	2.4, 2.7
M	Pro C$^\gamma$H(pro-*S*)–Pro C$^\delta$H(pro-*S*)	0.23	2.3[d]
N	Pro C$^\gamma$H(pro-*R*)–Pro C$^\delta$H(pro-*S*)	0.24	2.9[d]
O	boroArg C$^\alpha$H–boroArg C$^\beta$H^2 [c]	0.26, 0.26	2.2
P	boroArg C$^\alpha$H–boroArg C$^\beta$H^3 [c]	0.21	2.5, 2.6

[a] The correlation times, τ_c, were calculated from eq 8. Pairs of values were obtained when both (*i*,*j*) and (*j*,*i*) crosspeaks for the NOESY and ROESY were symmetrical, otherwise only one was used. [b] The range of interproton distances for each vector was calculated from eqs 6 and 7 using τ_c for that proton pair. [c] This geminal pair has not been stereospecifically assigned. [d] The resulting data pair was not symmetrical for this vector, so the most reasonable value was used. The value of τ_c for the proton pair "F" is anomalous and maybe artifactual. [e] Column 1 gives the letter designations for each proton pair. Our model of the structure of I was obtained by energy minimization using the distance constrains in column 4 (Figure 5A). For comparison, the structure of H-(D)Phe-Pro-ArgCH$_2$Cl bound in the active site of thrombin[8] was shown (Figure 5B). For documentation, the letter designation for individual proton pairs is given with distances in angstroms in parentheses. The first distance is for the energy-minimized structure and the second (in italics) is for the crystal structure: A (2.5, *2.5*), B (2.6, *2.6*), C (2.5, *2.3*), D (2.9, *2.8*), E (1.8, *1.8*), F (3.8, *4.2*), G (2.3, *2.1*), H (2.5, *2.2*), I (4.3, *3.7*), J (3.5, *4.1*), K (1.8, *1.8*), L (2.3, *2.2*), M (2.4, *2.3*), N (2.8, *3.0*).

the zero-shielding region.[18] We deduce from the calculations of Bovey[19] that Pro C$^\delta$H(*pro-R*) is 3–5 Å from the center of the aromatic ring.

Interproton distances calculated from ROESY and NOESY data (Table IV) define the structure of the -(D)Phe-Pro- portion of **I**. The interproton distances of the energy-minimized solution structure are consistent with those measured to within 0.3 Å (see Table IV, footnotes).

Finally, solution dynamics are consistent with our model. Values of the correlation times, τ_c, reflect the mobility of proton pairs. Consistent values of τ_c, between rigid structures such as the proline ring protons and the proton pairs arising from secondary structure, dissuade many criticisms of structural assignments based on experimental NOE and ROE data as discussed earlier. Correlation times for the proline ring proton pairs are 0.22–0.27 ns, similar to those for the Phe C$^\delta$H–Pro C$^\delta$H pairs (0.23–0.24 ns). Values of 0.18–0.22 ns were observed for the Phe C$^\alpha$H–Pro C$^\delta$H pairs. Greater mobility was observed for the Phe ring protons. For the interaction of the Phe C$^\beta$H and the ring protons, values of τ_c are 0.14–0.18 ns while for the intraring protons, 0.08 ns was measured. We can envision a 180° rotation of the phenyl ring in which the jump is effectively instantaneous. This would allow the Phe C$^\delta$H–Pro C$^\delta$H dipolar interactions to be preserved relative to those between ring protons, explaining the much lower values of τ_c for the latter.

Structural Stability. Stacking of the two ring system and the resulting structure probably arises from stabilization by π–π interactions between the edge of the phenyl ring and the (D)Phe-Pro amide bond. This is due to the attraction of the positively charged core of the aromatic ring to the delocalized π electrons of the amide bond as described by Hunter and Sanders.[20] Small temperature coefficients, –0.5 and 1.6 ppb/K, for Pro C$^\delta$H(*pro-R*) and Pro C$^\delta$H(*pro-S*), and small solvent effects on the chemical shift indicate that the solution structure is highly stable. The solvent perturbations for Pro C$^\delta$H(*pro-R*) and Pro C$^\delta$H(*pro-S*) are comparable to those observed for the pyridyl C_2 and C_4 protons in the nucleotides NADH and NAD, where intramolecular interactions between the adenyl and pyridyl rings are due also to π–π interactions.[21]

Concluding Remarks. Our observation that -(D)Phe-Pro- peptides have secondary structure is surprising in light of the work of Mierke et al.[22] They found that even after cyclization, the biologically active conformation of somatostatin may be only one of a large ensemble of conformations. However, Feinstein et al.[23] and Imperiali and Shannon[24] have shown that secondary structure may be adopted by acyclic peptides in aqueous solution, and the latter group have also demonstrated correlations with biological activity. Recently, Rich[25] reported that argatroban, a thrombin inhibitor consisting of an arginyl residue, an aromatic ring, and a piperidyl ring, has a secondary structure in aqueous solution that resembles its conformation bound to thrombin. He also compares this result with similar properties observed for cyclosporin. In both cases, the solution structure is attributed to hydrophobic interactions defined as "hydrophobic collapse". These studies and our observation for the -(D)Phe-Pro- peptides suggest that solution structures for small peptide analogs are fairly common and that they may arise from several different types of interaction. Clearly this phenomenon is an important consideration in the design of small molecules to bind to biological receptors.

Experimental Section

The temperature throughout all the experiments was controlled at 298 K, except where otherwise noted.

NMR Spectroscopy. The samples **I–IV** (see Scheme I and Table I), were dissolved in 99.996% deuterium oxide (D_2O) (MSD Isotopes) to various concentrations (1–80 mM) at various pH values (1–6). Solutions in methanol-d_4 (CD_3OD), deuteriochloroform ($CDCl_3$), and DMSO-d_6 were similarly prepared. For the NOE experiments, the solutions were freshly degassed by the freeze–thaw–pump procedure. Exchangeable protons were observed in samples dissolved in 80/20 H_2O/D_2O solutions at pH 6. ^1H-NMR spectra were initially recorded on General Electric QE-300 and Varian VXR-500 spectrometers, and further experiments were performed on a Bruker AMX600.

Coupling Constant Analysis. Peak splittings were measured at 293, 333, and 353 K. The dihedral angles were calculated using the equation of Karplus[15]

$$^3J = A\cos^2\theta + B\cos\theta + C \quad (1)$$

where $\theta = \Phi - 60°$ for $^3J_{HN\alpha}$, $\theta = \chi_1 - 120°$ for Hβ_2, and $\theta = \chi_1$ for Hβ^3, as defined by IUPAC-IUB.[26] The values of *A*, *B*, and *C* were 6.4, –1.4, and 1.9 for $^3J_{HN\alpha}$,[27] and 9.5, –1.6, and 1.8 for $^3J_{\alpha\beta}$.[28]

The coupling constants were analyzed in terms of three staggered conformations about the Cα–Cβ bond, using 4.1, 12.0, 2.1, 11.7, 2.9, and 4.7 Hz[18] as the reference values for J_g(Hα-Hβ^2), J_t(Hα-Hβ^3), J_g(Hα-Hβ^3), J_t(Hα-Hβ^2), $J_{g'}$(Hα-Hβ^2), and $J_{g'}$(Hα-Hβ^3), respectively, for the equations

$$^3J_{\alpha\beta 2} = P_I J_g(H\alpha\text{-}H\beta^2) + P_{II} J_t(H\alpha\text{-}H\beta^2) + P_{III} J_{g'}(H\alpha\text{-}H\beta^2) \quad (2)$$

$$^3J_{\alpha\beta 3} = P_I J_t(H\alpha\text{-}H\beta^3) + P_{II} J_g(H\alpha\text{-}H\beta^3) + P_{III} J_{g'}(H\alpha\text{-}H\beta^3) \quad (3)$$

where P_I, P_{II}, and P_{III} are populations of the rotamers **I**, **II**, and **III** in Figure 3.

Correlation Time and Interproton Distance Calculations. The optimum mixing time of 600 ms for the 2D NOESY[29] and ROESY[30] experiments was determined by measuring the intensities of rotating frame NOEs A_{RF} and longitudinal NOEs $A_{||}$ in 1D NOESY and ROESY experiments at 600 MHz. NOESY and ROESY data were acquired with identical recycling and mixing times (5 and 0.6 s, respectively), temperature (298 K), and concentration of **I** (2.5 mM). Peak intensities were obtained from volume integration. The intensities of the ROESY peaks were adjusted for the spin-lock field offset using the method of Griesinger and Ernst[31] to obtain the corrected absorption matrix A'_{RF}. The corrected NOESY and ROESY spectra were then backtransformed to the corresponding relaxation matrices $\mathbf{R}_{RF}$ and $\mathbf{R}_{||}$ according to the chemical exchange equation of Jeener et al.[29] adapted for cross relaxation by Macura and Ernst:[32]

$$\mathbf{A} = e^{-\mathbf{R}t_m} \quad (4)$$

where t_m is the mixing time. This approach corrects for spin diffusion effects where off-diagonal elements in **R** represent cross relaxation rates, $(\sigma)_{ij}$, between pairs of nonequivalent spins.

The measured cross relaxation rates $(\sigma_{RF})_{ij}$ obtained from the ROESY experiment were corrected to true transverse cross relaxation rates $(\sigma_\perp)_{ij}$ by eq 5:[4,31]

$$(\sigma_\perp)_{ij} = [\sqrt{(\omega_1^2 + \Delta_i^2)}\sqrt{(\omega_1^2 + \Delta_j^2)}(\sigma_{RF})_{ij} - \Delta_i^2\Delta_j^2(\sigma_\parallel)_{ij}]/\omega_1 \quad (5)$$

where Δ_j and Δ_i are the offsets of spins i and j from the carrier, and ω_1 is the spin-lock field. Columns of spin j in both rate matrices, $\mathbf{R}_{RF}$ and $\mathbf{R}_{||}$, were multiplied by the number of protons contributing to that spin to maintain the true matrix symmetry.

The interproton distance $(r)_{ij}$ is related to the cross relaxation rate $(\sigma)_{ij}$ as follows:

$$(\sigma_\perp)_{ij} = \frac{\gamma^4 h^2 \tau_c}{10(r)_{ij}^6}\left(\frac{3}{1+\omega_0^2\tau_c^2} + 2\right) \quad (6)$$

$$(\sigma_\parallel)_{ij} = \frac{\gamma^4 h^2 \tau_c}{10(r)_{ij}^6}\left(\frac{6}{1+4\omega_0^2\tau_c^2} - 1\right) \quad (7)$$

where γ is the ^{1}H gyromagnetic ratio, h is Planck's constant, ω_o is the spectrometer frequency for ^{1}H, and τ_c is the correlation time. Solving eq 6 and 7 simultaneously, τ_c is expressed independently of $(r)_{ij}$:

$$(1 + 2R_{ij})x^2 + (22R_{ij} - 1)\,x + 5\,(R_{ij} - 1) = 0 \quad (8)$$

where $R_{ij} = (\sigma_\parallel)_{ij}/(\sigma_\perp)_{ij}$ and $x = \omega_o^2\tau_c^2$. The interproton distance $(r)_{ij}$ was calculated using the resulting values of τ_c.

Energy Minimization. The molecular dynamics and energy minimizations were performed with the *Discovery* program[33] within *InsightII* (Biosym) on a Personal Iris workstation (Silicon Graphics). Various starting structures for minimization were obtained by sampling from the molecular dynamics simulations carried out for 1 ps at 600 K, sampling every 100 fs with a step size of 1 fs. Conformations of **I** were minimized with the conjugate gradient algorithm for 10 000 iterations and a scalar dielectric constant of 80, employing distances calculated as above. These distance restraints, given as the pairs B, C, D, F, G, H, I, J, L, M, and N in Table IV, were applied with equal and constant pulling forces, with the upper and lower limits, as pull and push distances, respectively. Where only one distance was calculated, 0.1 Å was added or subtracted from the limits. After minimization with restraints until the derivative was 0.001, the restraints were removed and the minimization repeated.

Enzyme Assays. Peptide boronic acids were prepared and evaluated as inhibitors of thrombin by the procedures we have described previously.[3]

Acknowledgment. We thank Peter Domaille for his valuable advice on the NMR experiments and for his backtransformation program. We would like to express our appreciation to Lawrence Mersinger for his excellent technical expertise. We also thank P. C. Weber for sharing X-ray crystal data with us, Dawn Ruble and Zixia Feng for assistance in molecular graphics, Nick Hodge for the use of the molecular modeling facility, and Sheng-Lian Lee, Lynn Abell, Michael Levitt, and Mark Nelson for reading the manuscript.

Supplementary Material Available: Tables of NOESY and ROESY absorption matrices $A_{||}$ and A_{RF}, corrected ROESY intensities A'_{RF}, and longitudinal, rotating frame, and transverse relaxation matrices, $\mathbf{R}_{||}$, $\mathbf{R}_{RF}$, and $\mathbf{R}_\perp$ (6 pages). Ordering information is given on any current masthead page.

References

(1) The prefix "boro" of boroArg indicates that the carbonyl of the amino acid residue is replaced by $B(OH)_2$; the systematic name for arginine boronic acid would be (1-amino-4-guanidinobutyl)boronic acid (see Scheme I). Other abbreviations are Ac, acetyl; Boc, *tert*-butyloxycarbonyl; COSY, two-dimensional correlation spectroscopy; NOE, nuclear Overhauser enhancement; NOESY, two-dimensional nuclear Overhauser spectroscopy; ppm, parts per million; ROE, NOEs measured in rotating frame experiments; ROESY, rotating-frame NOESY; TOCSY, total correlation spectroscopy.

(2) Schechter, I.; Berger, A. On the Size of the Active Site in Proteases. I. Papain. *Biochem. Biophys. Res. Commun.* **1967**, *27*, 157–162.

(3) Kettner, C.; Mersinger, L. M.; Knabb, R. Selective Inhibition of Thrombin by Peptides of BoroArginine. *J. Biol. Chem.* **1990**, *30*, 18289–18297.

(4) Davis, D. G. A Novel Method for Determining Internuclear Distances and Correlation Times from NMR Cross-Relaxation Rates. *J. Am. Chem. Soc.* **1987**, *109*, 3471–3472.

(5) (a) Kettner, C.; Shaw, E. D-Phe-Pro-ArgCH$_2$Cl—A Selective Affinity Label for Thrombin. *Thromb. Res.* **1979**, *14*, 969–973. (b) Kettner, C.; Shaw, E. Inactivation of Trypsin-Like Enzymes with Peptides of Arginine Chloromethyl Ketone. *Methods Enzymol.* **1981**, *80*, 826–841. (c) Bajusz, S.; Barabas, E.; Tolnay, P.; Szell, E.; Bagdy, D. Inhibition of Thrombin and Trypsin by Tripeptide Aldehydes. *Int. J. Pept. Protein Res.* **1978**, *12*, 217–221. (d) Bajusz, S.; Szell, E.; Bagdy, G.; Harvath, G.; Diozegi, D.; Fittler, Z.; Szabo, G.; Juhasz, A.; Szilagyi, G. Highly Active and Selective Anticoagulants: D-Phe-Pro-Arg-H, a Free Tripeptide Aldehyde Prone to Spontaneous Inactivation, and Its Stable N-Methyl Derivative, D-MePhe-Pro-Arg-H. *J. Med. Chem.* **1990**, *33*, 1729–1735. (e) Claeson, G.; Aurell, L. Small Synthetic Peptides with Affinity for Proteases in Coagulation and Fibrinolysis, An Overview. *Ann. N.Y. Acad. Sci.* **1981**, *370*, 798–811.

(6) Knabb, R. M.; Kettner, C. A.; Timmermans, P. B. M. W. M.; Reilly, T. M. In Vivo Characterization of a New Synthetic Thrombin Inhibitor. *Thromb. Haemostas.* **1992**, *67*, 56–59.

(7) Hussain, M. A.; Knabb, R.; Aungst, B. J.; Kettner, C. Anticoagulant Activity of a Peptide Boronic Acid Thrombin Inhibitor by Various Routes of Administration in Rats. *Peptides* **1991**, *12*, 1153–1154.

(8) Bode, W.; Mayr, I.; Baumann, U.; Huber, R.; Stone, S. R.; Hofsteenge, J. The Refined 1.9 Å Crystal Structure of Human α-Thrombin: Significance of the Tyr-Pro-Pro-Try Insertion Segment. *EMBO J.* **1989**, *193*, 3467–3475.

(9) Bachovchin, W. W.; Wong, W. Y. L.; Farr-Jones, S.; Shenvi, A. B.; Kettner, C. A. ^{15}N NMR Spectrometry of the Active-Site Histidyl Residue of Serine Proteases in Complexes Formed with Peptide Boronic Acids Inhibitors. *Biochemistry* **1988**, *27*, 7689–7697.

(10) Bone, R.; Frank, D.; Kettner, C. A.; Agard, D. A. Structural Analysis of Specificity: α-Lytic Protease Complexes with Analogues of Reaction Intermediates. *Biochemistry* **1989**, *28*, 7600–7609.

(11) Weber, P. C. unpublished results.

(12) Page, M. I.; Jencks, W. P. Entropic Contributions to Rate Accelerations in Enzymatic and Intramolecular Reactions and the Chelate Effect. *Proc. Natl. Acad. Sci. U.S.A.* **1971**, *68*, 1678–1683.

(13) Hruby, V. J. A Perspective on the Application of Physical Methods to Peptide Conformational-Biological Activity Studies. In *The Peptides*; Udenfriend, S., Meienhofer, J., Hruby, J. V., Eds.; Academic Press, Inc.: New York, 1985; Vol. 7, pp 1–14.

(14) Gierasch, L. M.; Rockwell, A. L.; Thompson, K. F.; Briggs, M. S. Conformation-Function Relationships in Hydrophobic Peptides: Interior Turns and Signal Sequences. *Biopolymers* **1985**, *24*, 117–135.

(15) Karplus, M. Interpretation of the Electron-Spin Resonance Spectrum of the Methyl Radical. *J. Chem. Phys.* **1959**, *30*, 11–15.

(16) Feeney, J. Improved Component Vicinal Coupling Constants for Calculating Side-Chain Conformations in Amino Acids. *J. Magn. Reson.* **1976**, *21*, 473–478.

(17) Wuthrich, K. *NMR of Proteins and Nucleic Acids*; Wiley Interscience: New York, 1986; p 17.

(18) Johnson, C. E.; Bovey, F. A. Calculation of Nuclear Magnetic Resonance Spectra of Aromatic Hydrocarbons. *J. Chem. Phys.* **1958**, *29*, 1012–1014.

(19) Bovey, F. A. *Nuclear Magnetic Resonance Spectroscopy*; Academic Press: New York, 1969; Appendix C.

(20) Hunter, C. A.; Sanders, J. K. M. The Nature of π–π Interactions. *J. Am. Chem. Soc.* **1990**, *112*, 5525–5534.

(21) Catteral, W. A.; Hollis, D. P.; Walter, C. F. Nuclear Magnetic Resonance Study of the Conformation of Nicotinamide-Adenine Dinucleotide and Reduced Nicotinamide-Adenine Dinucleotide in Solution. *Biochemistry* **1969**, *8*, 4032–4036.
(22) Mierke, D. F.; Pattaroni, C.; Delaet, N.; Toy, A.; Goodman, M.; Tancredi, T.; Motta, A.; Temussi, P. A.; Moroder, L.; Bovermann G.; Wunsch, E. Cyclic Hexapeptides Related to Somatostatin. *Int. J. Pept. Protein Res.* **1990**, *36*, 418–432.
(23) Feinstein, R. D.; Polinsky, A.; Douglas, A. J.; Beijer, C. M. G. F.; Chadha, R. K.; Benedetti, E.; Goodman, M. Conformational Analysis of the Dipeptide Sweetener Alitame and Two Stereoisomers by Proton NMR, Computer Simulations, and X-ray Crystallography. *J. Am. Chem. Soc.* **1991**, *113*, 3467–3473.
(24) Imperiali, B.; Shannon, K. L. Differences Between Asn-Xaa-Thr-Containing Peptides: A Comparison of Solution Conformation and Substrate Behavior with Oligosaccharyltransferase. *Biochemistry* **1991**, *30*, 4374–4380.
(25) Rich, D. H. Effect of Hydrophobic Collapse on Enzyme-Inhibitor Interations. Implications for the Design of Peptidomimetics. In *Perspectives in Medicinal Chemistry*; Testa, B., Kyburz, E., Fuhrer, W., Giger, R., Eds.; Verlag Helvetica Chimica Acta; Basel, 1993; pp 15–25.
(26) IUPAC–IUB Commission on Biochemical Nomenclature Abbreviations and Symbols for the Description of the Conformation of Polypeptide Chains. *J. Mol. Biol.* **1970**, *52*, 1–17.
(27) Pardi, A.; Billeter, M.; Wuthrich, K. Calibration of the Angular Dependence of the Amide Proton-C^{α} Proton Coupling Constants, $^{3}J_{HN\alpha}$, in a Globular Protein. *J. Mol. Biol.* **1984**, *180*, 741–751.
(28) DeMarco, A.; Llinas, M.; Wuthrich, K. Analysis of the 1H-NMR Spectra of Ferrichrome Peptides. I. The Non-Amide Protons. *Biopolymers* **1978**, *17*, 617–636.
(29) Jeener, J.; Meier, B. H.; Bachman, P.; Ernst, R. R. Investigation of Exchange Processes by Two-Dimensional NMR Spectroscopy. *J. Chem. Phys.* **1979**, *71*, 4546–4553.
(30) (a) Bothner-By, A. A.; Stephens, R. L.; Lee J.-M.; Warren, C. D.; Jeanloz, R. W. Structural Determination of a Tetrasaccharide Transient Nuclear Overhauser Effects in the Rotating Frame. *J. Am. Chem. Soc.* **1984**, *106*, 811–813. (b) Bax, A.; Davis, D. G. Practical Aspects of Two-Dimensional Transverse NOE Spectroscopy. *J. Magn. Reson.* **1985**, *63*, 207–213.
(31) Griesinger, C.; Ernst, R. R. Frequency Offset Effects and Their Elimination in NMR Rotating-Frame Cross-Relaxation Spectroscopy. *J. Magn. Reson.* **1987**, *75*, 261–271.
(32) Macura, S.; Ernst, R. R. Elucidation of Cross Relaxation in Liquids by Two-Dimentional N. M. R. Spectroscopy. *Mol. Phys.* **1980**, *41*, 95–117.
(33) Hagler, A. T. Theoretical Simulation of Conformation, Energetics, and Dynamics of Peptides. In *The Peptides*; Udenfriend, S., Meienhofer, J., Hruby, J. V., Eds.; Academic Press, Inc.: New York, N.Y., 1985; Vol. 7, pp 214–296.
(34) Bothner-By, A. A.; Castellano, S. M. In *Computer Programs for Chemistry*; De Tar, D. F., Ed.; Benjamin Press, New York, 1968; Vol. 1, pp 10–15.
(35) Aue, W. P.; Bartholdi, E.; Ernst, R. R. Two-Dimensional Spectroscopy. Application to Nuclear Magnetic Resonance. *J. Chem. Phys.* **1976**, *64*, 2229–2246.